JOURNAL OF MATERIALS SCIENCE 29 (1994) 4075–4080

A bioactive composite material produced by the sol–gel method

S. M. JONES, S. E. FRIBERG
Center for Advanced Material Processing, Department of Chemistry, Clarkson University, Potsdam, NY 13676, USA

J. SJÖBLOM
Department of Chemistry, University of Bergen, N-5007 Bergen, Norway

The interaction of sol–gel derived glass/organic polymer composite gel monoliths, containing a calcium salt, with an ambient solution of simulated body fluid was investigated. These gels were aged, wetted, placed in simulated body fluid, and then observed with a scanning electron microscope. The chemical compositions of the sample and the apatite were determined by energy dispersive X-ray analysis. A calcium phosphate apatite layer was clearly observed after 7 days, as was an intermediate layer which included not only calcium and phosphate in its composition but also silicon. Calcium and phosphate were also observed to be present in the outer layer of the sample, presumably having precipitated on the external surfaces of the pores in the SiO_2 network.

1. Introduction

The search for innovative biomaterials, specifically bone implants, received new impetus in the early 1970s when Hench *et al.*, introduced Bioglass^R [1]. Bioglass^R was shown to be bioactive, i.e. a calcium phosphate apatite layer formed on its surface from the ions present in the surrounding solution, when placed *in vivo*. Since that time, various other glasses and glass-ceramics, such as Ceravital^R [2], sintered hydroxyapatite ceramic [3], and apatite and wollastonite containing (A–W) glass-ceramic [4], have been shown to be bioactive. The formation of an apatite layer on these materials is crucial to their employment as biological implants, in that the apatite acts as a structural bond between the implant and the bone into which it is placed [5–8].

The sol–gel method provides a viable alternative to the classical processing methods of glass-ceramics and therefore to the production of bioactive materials [9–15]. In the sol–gel method, a metal alkoxide, e.g. tetraethoxysilane (TEOS), undergoes hydrolysis in the presence of water with an acid or base catalyst. The silanols produced then condense forming an SiO_2 network. The network dries as the ethanol produced and the water present evaporate, gradually shrinking to form a porous glass-like gel [16–18]. The advantages of the sol–gel method are the processing latitudes available and the fact that the processing is done at room temperature.

Because the processing is carried out at room temperature, and does not involve elevated temperatures of several hundred degrees, as are used in classical glass-ceramic sintering, organic compounds can be introduced at the initial stages and become an integral component of the resultant gel. Organically modified silicates can be formed by introducing a monomer to the initial metal alkoxide solution and subsequently polymerizing it, resulting in a hybrid silicate/polymeric network [19–24]. This process has been used to produce composites with a Young's modulus very close to that of borosilicate glass [25]. Furthermore, the organics introduced need not be a component of the network; they could be proteins such as human growth hormone, osteopontin, or osteocalcin which would play an active role in promoting the formation of new bone tissue when present in an implanted material.

The interaction of implanted materials and the ions in bodily fluids has been found to be crucial in the process of bioactive implant incorporation. The exchange of various ions between the implanted material and the ambient solution is pivotal to the formation of an intermediate apatite layer bridging the implant and the bone. SiO_2–CaO glass-ceramics have exhibited a finite solubility of the network when placed in bodily fluids, either *in vivo* or *in vitro*. This solubility produces two effects: (1) a silica-rich gel phase is established at the exterior surfaces of the implanted material, and (2) the local concentration of calcium around the implant is greater than that found in the bulk solution [5, 7, 26–28]. The solubility of silicon produces a flexible and more thoroughly hydrated network which lends itself to the subsequent formation of a calcium phosphate apatite. The increased local concentration of calcium enhances the likelihood of the complexation of calcium and phosphorus into an apatite structure.

Owing to the fact that a hydrophilic gel network is formed when the sol–gel method is employed and the processing advantages realized by this method, it

0022–2461 © *1994 Chapman & Hall*

seemed extremely promising that sol–gel derived bioactive materials could be produced. By varying the precursor concentrations of alkoxide and water the network produced can be tailored to optimize its interaction with the ambient environment. The local concentration of ions such as calcium can be influenced by the initial inclusion of inorganic salts of calcium which will later elute when the sample is placed in an aqueous environment.

2. Experimental procedure

2.1. Materials

Tetraethoxysilane (Aldrich), methylmethacrylate (MMA) (Kodak), 2,2′-azo*bis*(2-methyl propionitrile) (Kodak), $CaCl_2 \cdot H_2O$ (Mallinckrodt, analytical reagent), HNO_3 (Fisher, Reagent A.C.S.), $MgCl_2 \cdot 6H_2O$ (Mallinckrodt, analytical reagent), $NaHCO_3$ (J. T. Baker, Baker Analysed Reagent), K_2HPO_4 (J. T. Baker, Baker Analysed Reagent), NaCl (J. T. Baker, Baker Analysed Reagent), KCl (Fisher, Certified A.C.S.), HCl (Fisher, Reagent A.C.S.), and trishydroxymethyl-aminomethane (J. T. Baker, Baker Analysed Reagent) were all used as-received.

2.2. Preparation of gel monoliths

TEOS and solutions of 10%–20% $CaCl_2$ (pH adjusted to 1 with HNO_3) were mixed on a vortexer until a transparent solution was obtained (2–3 min). To this was added methylmethacrylate and 2,2′-azo*bis* (2-methyl propionitrile), a polymerization initiator (see Table I). The sample tube was then sealed and the solution gradually condensed into a solid gel. After gelation the sample container cap was loosened allowing the interstitial liquid to evaporate. One week after gelation the samples were placed in an ultraviolet cabinet to polymerize the MMA.

Prior to placing the samples in simulated body fluid (SBF), which mimics human blood plasma, the surface of the gels were hydrated by placing them in an ambient atmosphere which was saturated with water vapour. This was necessary because the gels tend to crack due to the resultant interfacial pressures when a liquid is suddenly introduced to the pores in the silica network. The samples were then placed in SBF, which was prepared by dissolving reagent-grade NaCl, $CaCl_2$, $MgCl_2$, KCl, $NaHCO_3$, and K_2HPO_4 in deionized water. This solution was buffered at pH 7 with 50 mM trishydroxymethyl aminomethane and 45 mM HCl. The sample tubes were then thermostatted at 37 °C in a circulating water bath.

2.3. Surface analysis

The samples were removed from the SBF, cut with a scapel to reveal a cross-section of the material, air-dried for approximately 30 min and mounted on an aluminium stub. A Jeol model 6300 scanning electron microscope with a Noran Instruments Voyager X-ray microanalyser was used to observe and to obtain compositional analyses of the samples.

TABLE I Compositions (in grams) of sol–gel composite samples

Sample	TEOS	$H_2O/CaCl_2$	MMA
C_A87	1.208	0.300/10%	5%
C_A109	1.092	0.420/10%	10%
C_A128	0.810	0.695/20%	10%

3. Results

Fig. 1 shows a scanning electron micrograph of the interface between the initial sample, C_A128, and the apatite layer that formed after 7 days. Fig. 2 shows the varying composition of the sample and that of the apatite. It was clearly observed that prior to the actual interface between the sample and the apatite, calcium and phosphate are present in the SiO_2 matrix. The apatite layer is almost exclusively calcium phosphate and consists of 5–50 μm plates.

Fig. 3 shows a scanning electron micrograph of the interface formed by sample C_A109 after 7 days in SBF; not only is the initial material and the Ca–P apatite formed, but also an intermediate layer. The compositions of these different layers are illustrated in Fig. 4. As in Fig. 2, the sample is seen to increase in calcium phosphate content as the interface is approached. The intermediate layer is primarily calcium phosphate but is also silica-rich relative to the Ca–P apatite. It can also be seen that the presence of silicon increases as the outer apatite layer is approached. The Ca–P apatite is similar in composition to that of sample C_A128; however, it is much denser adjacent to the intermediate layer and the outer plates are 1–5 μm. The aberrant height of the oxygen peak in Fig. 4b is assumed to be an analysis error by the Voyager system. Fig. 5 shows a linescan across the different layers and clearly illustrates the compositional gradient of the various elements as one moves through the interfaces.

Fig. 6 shows a scanning electron micrograph of the apatite layer formed on sample C_A87 after 8 weeks. Fig. 7 shows that the silicon content is similar to that seen in Fig. 4c and d, but is constant across the section observed until the exterior is encountered. The Al peak is due to secondary scattering from the stub. However, the morphology of the apatite which formed is clearly different from that observed above. The

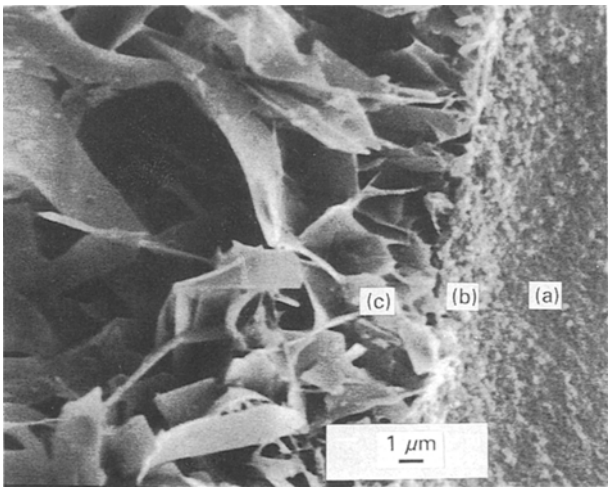

Figure 1 Scanning electron micrograph of sample C_A128 after 7 days in SBF showing the apatite layer formed on the sample surface.

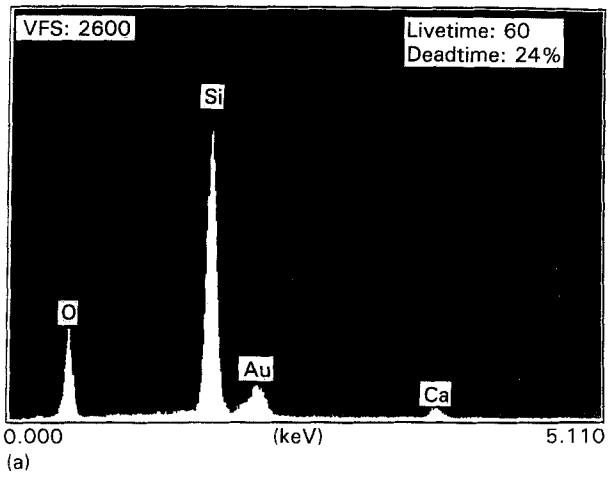

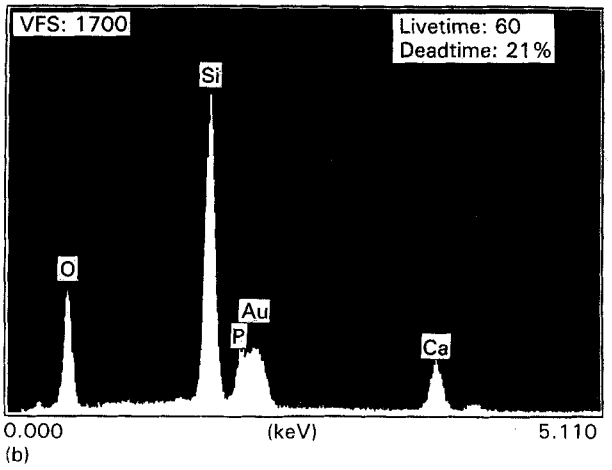

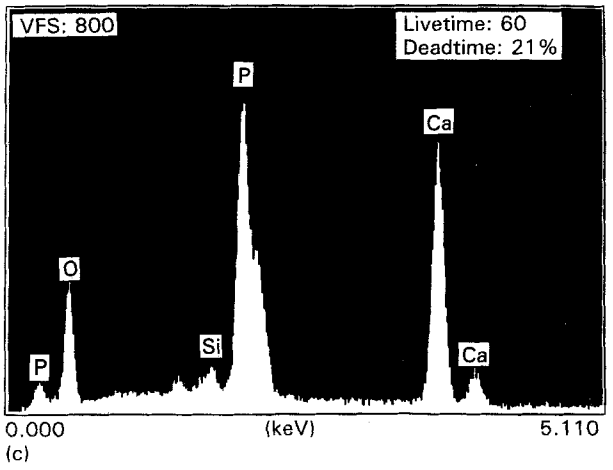

Figure 2 Energy dispersive X-ray spectra of sample C_A128; (a) inner sample region, (b) outer sample region, and (c) Ca–P apatite layer.

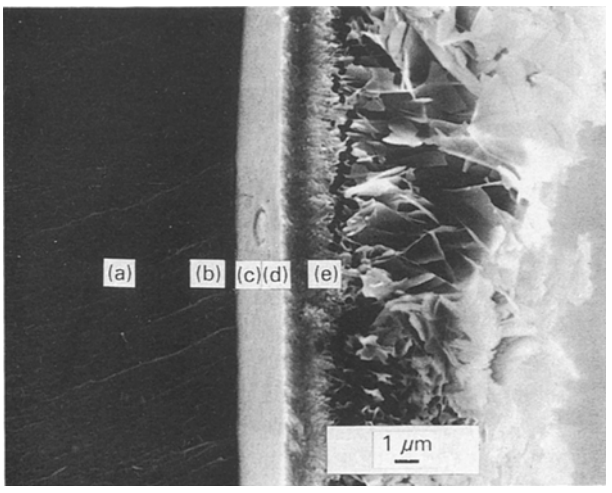

Figure 3 Scanning electron micrograph of sample C_A87 after 7 days in SBF showing the Ca–P apatite layer formed and an intermediate Ca–P–Si layer formed on the surface of the sample.

plates formed initially appear to have fused while additional apatite precipitated, forming a denser structure which is relatively rich in silicon throughout.

4. Discussion

The most ubiquitous aspect in the literature of the bioactivity of glasses is the formation of a silica gel layer at the surface of the glass sample [6–8, 26, 28–31]. It is generally agreed that this gel layer is formed by the dissolution of silicon and alkali ions present in the substrate [7, 32, 33]. The hydration of this layer then leads to the creation of nucleation sites for the apatite layer [26–29]. Andersson *et al.*, have proposed that the nucleation rate depends on the interfacial energy between the apatite and the substrate [28].

Kokubo proposed a mechanism for apatite formation in which silicon and calcium are released from the

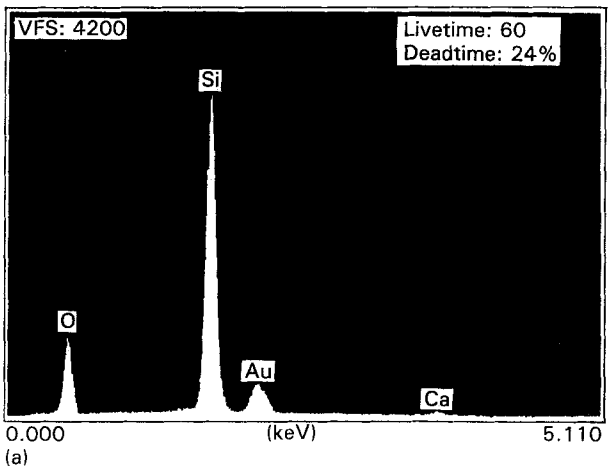

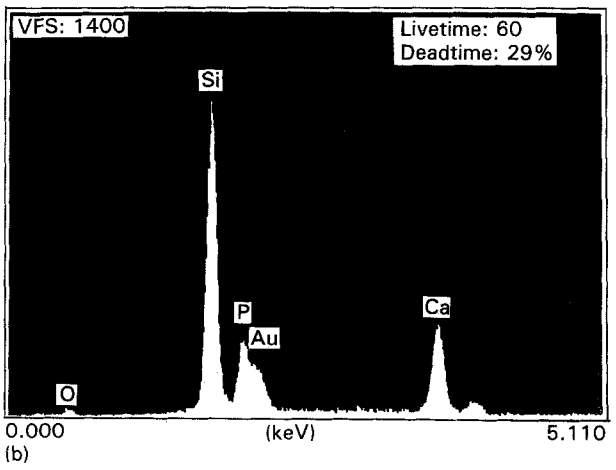

Figure 4 Energy dispersive X-ray spectra of sample C_A87; (a) inner sample region, (b) outer sample region, (c) intermediate Ca–P–Si apatite layer adjacent to sample, (d) intermediate Ca–P–Si apatite layer adjacent to Ca–P apatite, and (e) outer Ca–P apatite layer.

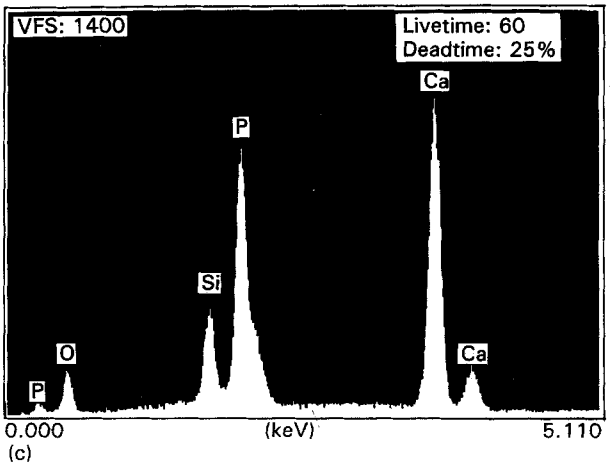

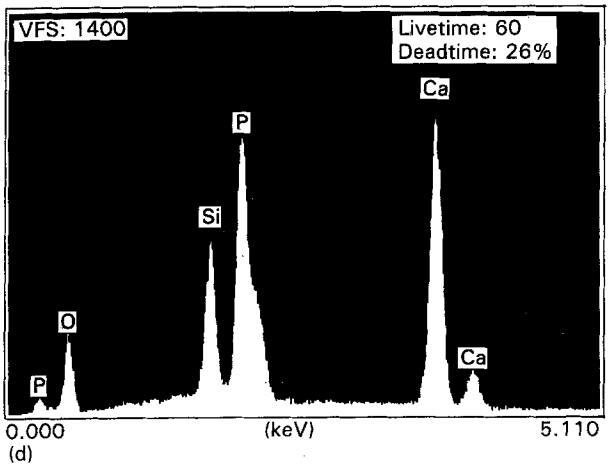

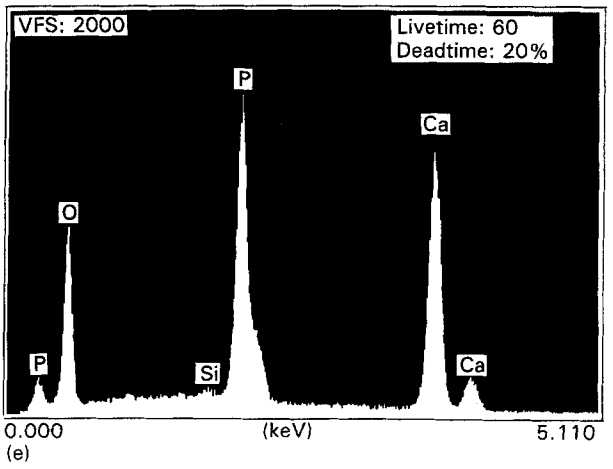

Figure 4 (continued).

glass and Ca–P apatite is then precipitated on to the surface [7]. However, the interaction between water and glass is a fairly complex process and a number of experimental parameters, e.g. pH, temperature, and the relative ion concentrations must be taken into consideration [34–37]. Andersson *et al.*, have recently proposed that apatite build-up is initiated by phosphorus complexation by the silica gel [26]. The materials studied here clearly show that P_2O_5-free glasses are bioactive and thus the source of the complexed phosphorus is the simulated body fluid [7, 29, 33].

From the differences in the initial precursor concentrations of samples C_A109 and C_A128 and the resultant apatite formed, certain proposals can be made. Because the mole ratios of H_2O/TEOS (denoted R)

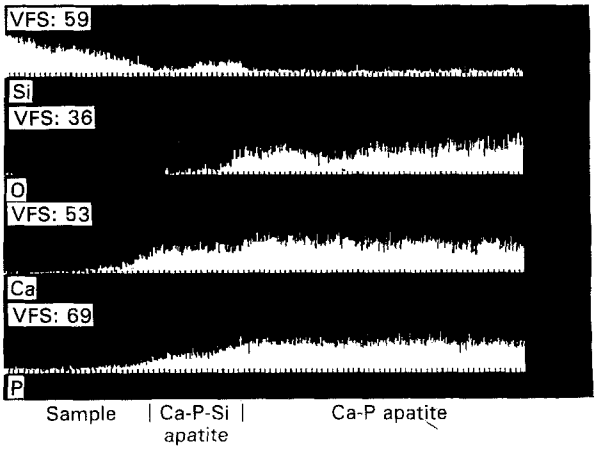

Figure 5 Energy dispersive X-ray linescan of sample C_A87 showing the relative amounts of Si, O, Ca, and P present in the sample and in the apatite layers. The scan begins at the far left and gradually moves through the apatite layers. VFS = vertical full scale.

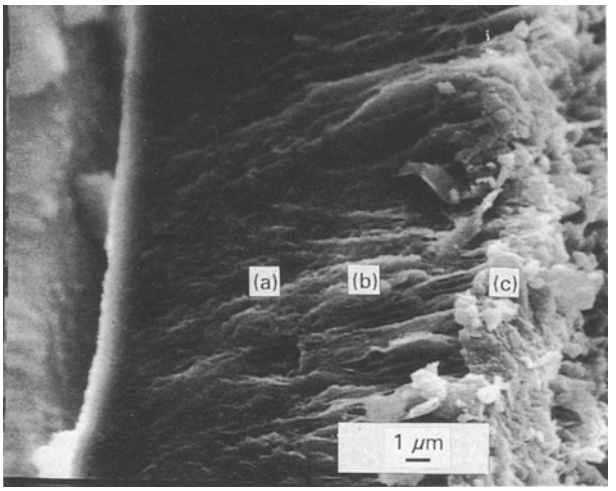

Figure 6 Scanning electron micrograph of sample C_A109 after 8 weeks in SBF showing the Ca–P–Si apatite layer formed.

were different, $R_{CA109} = 4$, $R_{CA128} = 9$, it is known that different gel networks were created [13, 38]. For the system with the higher R value the hydrolysis reaction will occur more rapidly and more completely. Incomplete hydrolysis of the alkoxides present generate fractal structures which can be simulated by a poisoned Eden growth model [39]. Keefer found that for systems in which the hydrolysis was more complete a surface fractal was formed, whereas for incomplete hydrolysis a mass fractal resulted, where mass fractals are those objects which have holes on every length scale [40]. Thus, the hydrolysed species for high R values will be rapidly incorporated into the forming clusters through reaction limited monomer-cluster growth, leading to a more polycondensed and less porous network [41–45]. From the discussion above, and this fact, the differences in the apatite layers formed may be explained.

The network of sample C_A128 led to limited silicon solubility and thus to Ca–P apatite formation directly on the surface of the glass. Calcium and phosphorus were observed to be present within the outer layer of the sample (see Fig. 2b), so nucleation occurred not

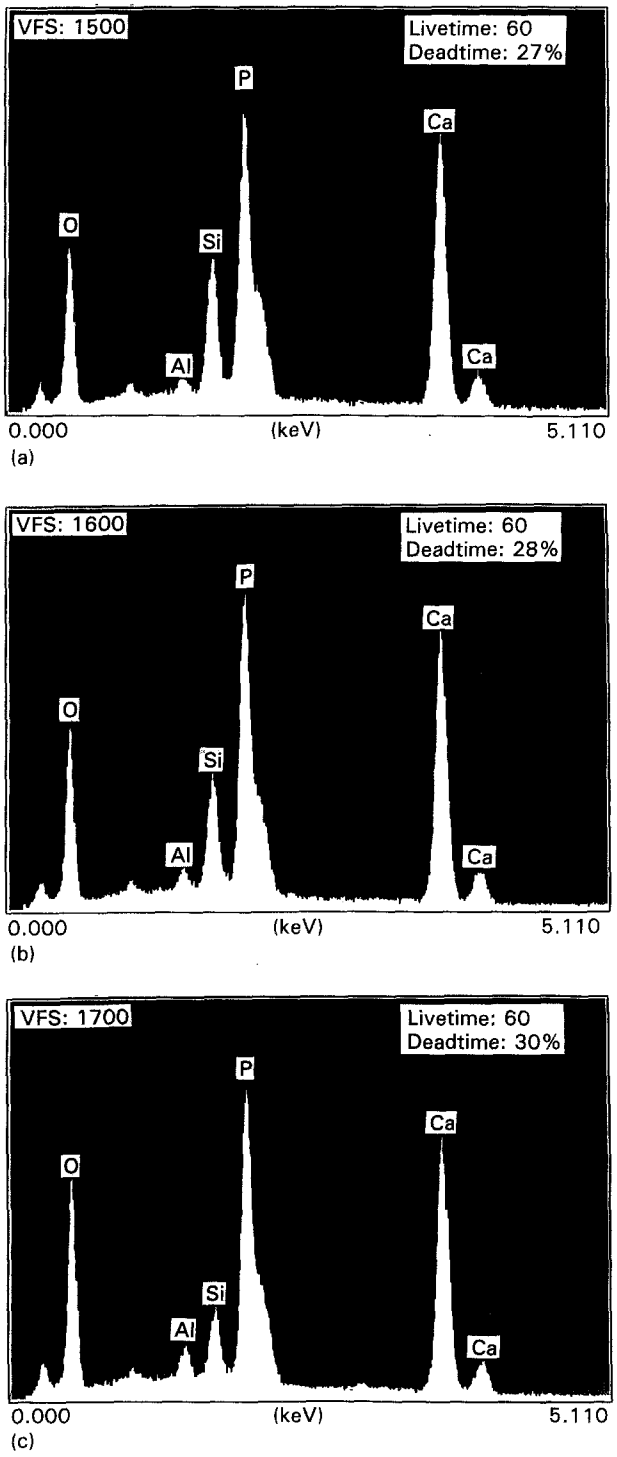

Figure 7 Energy dispersive X-ray spectra of sample C_A109; (a) inner Ca–P–Si apatite layer adjacent to sample, (b) outer Ca–P–Si apatite layer adjacent to Ca–P apatite, and (c) Ca–P apatite layer.

only on the surface but in the outer portions of the pores as well [8]. However, the calcium and phosphorus observed in the outer layer of sample C_A109 was greater than that for C_A128, (see Figs 2b and 4b), illustrating the difference in porosity of the two different networks.

The increased solubility of silicon for the more porous mass fractal network of sample C_A109 had a dramatic effect on the resultant apatite layer. The increased solubility led to a hydrated gel surface layer of very high surface area. Walker found that pure SiO_2 was bioactive if the surface area was sufficiently high, $> 400\,m^2\,g^{-1}$ [46]. It would also provide a large number of non-bridging oxygens which has been proposed as a prerequisite for apatite formation [28]. Owing to the availability of dissolved silicon in the immediate ambient solution, an apatite composed of complexed silicon, calcium and phosphorus formed on the surface of the sample. In calcium phosphate apatites it has been found that SiO_4 can replace PO_4 in the apatite structure [47]. This intermediate layer was markedly different from that of the outer Ca–P apatite; it is far denser and appears to be firmly bonded to the surface of the sample (see Fig. 3). Once the silicon in the ambient solution was complexed, a Ca–P apatite was formed; however, the plates are decidedly smaller and more closely packed.

The fact that complexation can continue until an extensive, dense structure results is illustrated in Fig. 6. The initial precursor composition of this sample is quite similar to that of C_A109, and thus it can be assumed that the initial stage of the formation of this apatite was quite similar to that of sample C_A109. The final composition of this apatite is intermediate to that of the inner and outer sections of the intermediate layer for sample C_A109, which may indicate continued dissolution and reprecipitation of the ions composing the apatite layer.

References

1. L. L. HENCH, L. L. SPLINTER, W. C. ALLEN and T. K. GREENLEE, *J. Biomed. Mater. Res. Symp.* **2** (1972) 117.
2. B. A. BLENKE, H. BROMER and K. DEUTSCHER, *Med. Ortho. Technol.* **95** (1975) 144.
3. M. JARCHO, J. F. KAY, K. I. GUMER, R. H. DOREMUS and H. P. DROMBECK, *J. Bioeng.* **1** (1977) 79.
4. T. KOKUBO, M. SHIGEMATSU, Y. NAGASHIMA, M. TASHIRO, T. NAKAMURA, T. YAMAMURO and S. HIGASHI, *Bull. Inst. Chem. Res. Kyoto Univ.* **60** (1982) 260.
5. W. VOGEL, W. HOLLAND, K. NAUMANN and J. GUMMEL, *J. Non-Cryst. Solids* **80** (1986) 34.
6. K. H. KARLSSON, K. FROBERG and T. RINGBOM, *ibid.* **112** (1989) 69.
7. T. KOKUBO, *ibid.* **120** (1990) 138.
8. L. L. HENCH, *J. Am. Ceram. Soc.* **74** (1991) 1487.
9. D. R. ULRICH, *J. Non-Cryst. Solids* **121** (1990) 465.
10. A. H. HEUER, D. J. FINK, V. J. LARAIA, J. L. ARIAS, P. D. CALVERT, K. KENDELL, G. L. MESSING, J. BLACKWELL, P. C. RIECKE, D. H. THOMPSON, A. P. WHEELER, A. VEIS and A. I. CAPLAN, *Science* **255** (1992) 1098.
11. W. HOLLAND, P. WAYNE, K. NAUMANN, J. VOGEL, G. CARL, C. JANA and W. GOTZ, *J. Non-Cryst. Solids* **129** (1991) 152.
12. L. L. HENCH and J. WILSON, in "Materials Research Society Symposium Proceedings", Vol. 180, edited by J. Brinker, D. E. Clark and D. R. Ulrich (Materials Research Society, Pittsburg, PA, 1990) p. 1061.
13. C. J. BRINKER and G. W. SCHERER, "Sol–Gel Science" (Academic Press, New York, 1990).
14. L. KLEIN (ed.), "Sol–Gel Technology For Thin Films, Fibers, Preforms, Electronics and Specialty Shapes" (Noyes, Park Ridge, NJ, 1988).
15. L. L. HENCH and J. K. WEST, *Chem. Rev.* **90** (1990) 33.
16. G. W. SCHERER, *J. Non-Cryst. Solids* **87** (1986) 199.
17. *Idem, ibid.* **91** (1987) 101.
18. *Idem*, in "Materials Research Society Symposium Proceedings", Vol. 121, edited by J. Brinker, D. E. Clark and D. R. Ulrich (Materials Research Society, Pittsburg, PA, 1988) p. 179.
19. H. SCHIMDT, *ibid.*, Vol. 32 (Materials Research Society, Pittsburg, PA, 1984) p. 327.

20. E. J. A. POPE and J. D. MACKENZIE, *ibid.* **32** (Materials Research Society, Pittsburg, PA, 1986) p. 809.
21. D. RAVAINE, A. SEMINEL, Y. CHARBOUILLOT and M. VINCENS, *J. Non-Cryst. Solids* **82** (1986) 210.
22. H. SCHIMDT, *ibid.* **112** (1989) 419.
23. H. SCHIMDT and H. WOLTER, *ibid.* **121** (1990) 428.
24. S. KOHJIYA, K. OCHIAI and S. YAMASHITA, *ibid.* **119** (1990) 132.
25. S. E. FRIBERG, C. C. YANG, M. B. BISCOGLIO and H. HELBIG, *J. Mater. Sci. Lett.* **11** (1992) 1373.
26. O. H. ANDERSSON, K. H. KARLSSON and K. KANGASNIEMI, *J. Non-Cryst. Solids* **119** (1990) 290.
27. O. H. ANDERSSON, G. LIU, K. H. KARLSSON, L. NIEMI, J. METTINEN and J. JUHANOJA, *J. Mater. Sci. Mater. Med.* **1** (1990) 219.
28. O. H. ANDERSSON and K. H. KARLSSON, *J. Non-Cryst. Solids* **129** (1991) 145.
29. C. OHTSUKI, T. KOKUBO and T. YAMAMURO, *ibid.* **143** (1992) 84.
30. C. Y. KIM, A. E. CLARK and L. L. HENCH, *ibid.* **113** (1989) 195.
31. K. OHURA, T. NAKAMURA, T. YAMAMURO, Y. EBISAWA, T. KOKUBO, Y. KOTOURA and M. OKA, *J. Mater. Sci. Mater. Med.* **3** (1992) 95.
32. C. OHTSUKI, T. KOKUBO and T. YAMAMURO, *ibid.* **3** (1992) 119.
33. Y. EBISAWA, T. KOKUBO, K. OHURA, T. YAMAMURO, *ibid.* **1** (1990) 239.
34. R. H. DOREMUS, *J. Non-Cryst. Solids* **48** (1982) 431.
35. H. SCHOLZE, *ibid.* **52** (1982) 91.
36. R. H. DOREMUS, Y. MEHROTRA, W. A. LANFORD and C. BURMAN, *J. Mater. Sci.* **18** (1983) 612.
37. H. DUNKEN and R. H. DOREMUS, *J. Non-Cryst. Solids* **92** (1987) 61.
38. J. C. POUXVIEL and J. P. BOILOT, *ibid.* **94** (1987) 374.
39. D. W. SCHAEFER and K. D. KEEFER, in "Materials Research Society Symposium Proceedings", Vol. 73 (Materials Research Society, Pittsburg, PA, 1986) p. 277.
40. K. D. KEEFER, *ibid.* p. 295.
41. C. J. BRINKER, K. D. KEEFER, R. A. SCHAEFER, R. A. ASSINK and B. D. KAY, *J. Non-Cryst. Solids* **63** (1984) 45.
42. C. J. POUXVIEL, J. P. BOILOT, J. C. BOLOIEL and J. Y. LALLAMAND, *ibid.* **89** (1987) 345.
43. C. J. BRINKER, K. D. KEEFER, D. W. SCHAEFER and C. S. ASHLET, *ibid.* **48** (1982) 47.
44. H. YANG, Z. DING and X. XU, *ibid.* **112** (1989) 449.
45. R. H. ASSINK and B. D. KAY, *ibid.* **99** (1988) 359.
46. M. M. WALKER, MS thesis, University of Florida, Gainsville, FL (1977).
47. C. KLEIN and C. S. HURLBUT, "Manual of Mineralogy" (Wiley, New York, 1977) p. 359.

Received 7 October 1992
and accepted 16 February 1994